Supp. Figure 1

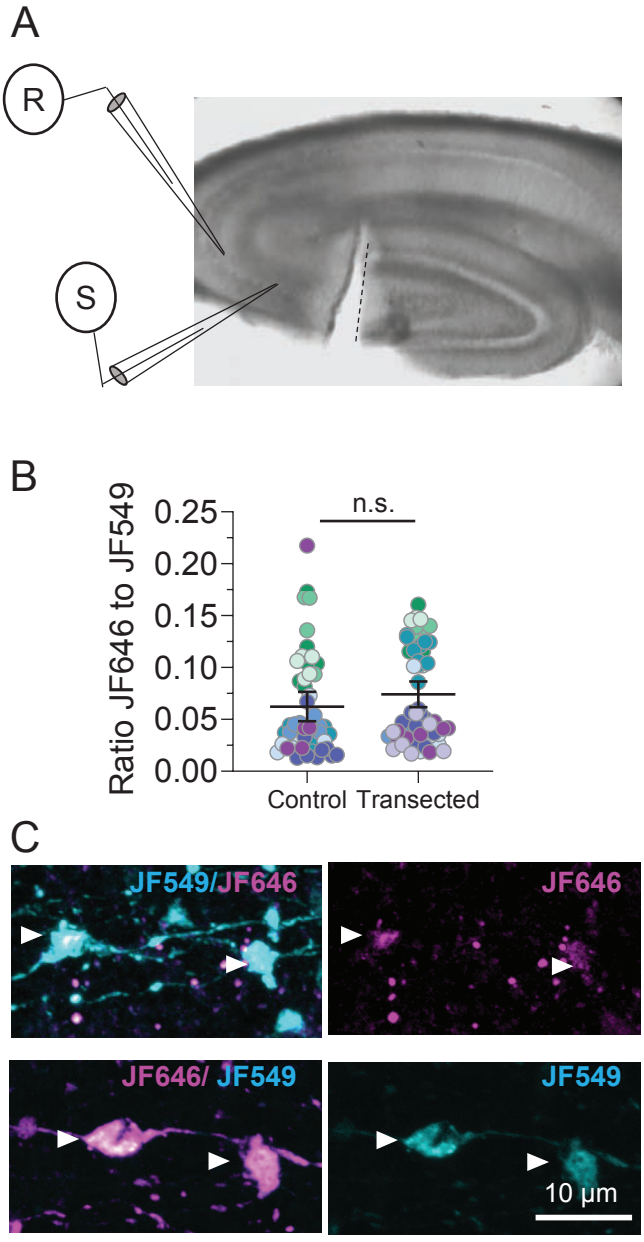

Supp. Figure 1. (related to Figure 1) MFBs synthesize Halo-actin locally A. Representative DIC fluorescence image of transected acute hippocampal slice showing recording configuration. **B.** Ratio of newly synthesized actin (JF646) to pre-existing actin (JF549) was not altered by transection. Control: 0.062 ± 0.007 v. Transected 0.074 ± 0.006 (Mean ± S.E.M.); Mann-Whitney, U = 1182, p = 0.08. n = 23 boutons, 8,7 slices respectively, 4 animals. Black line and bar represent the mean ± 95 % confidence interval. Points representing individual boutons are color-coded by slice and normalized to mean of Control. **C.** Reversing the order of the Halo dye did not affect labeling.

Supp. Figure 2

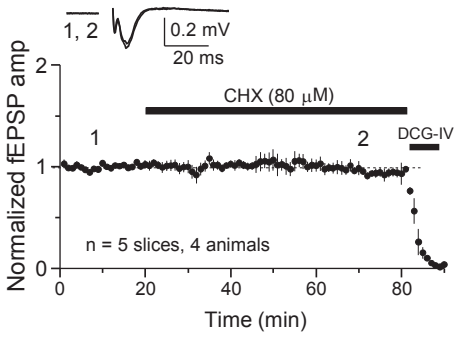

Supp Figure 2. (related to Figure 5) MF-LTP involves protein synthesis Electrophysiological recording from acute hippocampal slice demonstrating that CHX had no effect on baseline MF transmission with 1 hour of bath application. CHX: 0.935 ± 0.031; One sample t-test, p = 0.16.

Supp. Figure 3

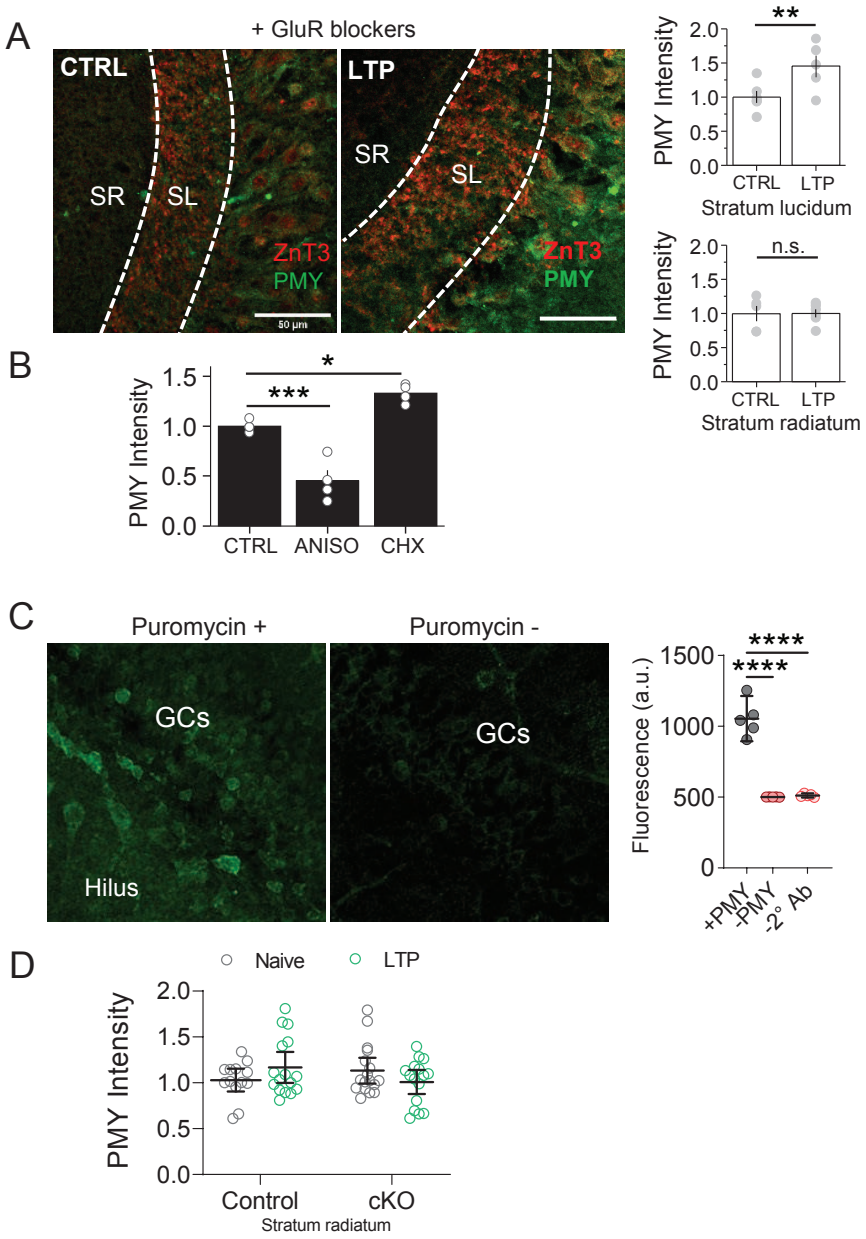

Supp. Figure 3. (related to Figure 6) Puromycin labeling in WT mice is increased with LTP A. LTP induction in the presence of blockers of ionotropic and metabotropic glutamate receptor blockers increased puromycin labeling (PMY) of newly synthesized proteins in MF tract (stratum lucidum) labeled with marker ZnT3, but not stratrum radiatum. (top) CTRL: 1.00 ± 0.09 v. LTP: 1.45 ± 0.16, Two-sample t-test, p = 0.027, (bottom) CTRL: 1.0 ± 0.11 v. LTP: 1.0 ± 0.06, Two-sample t-test, p = 0.98. n = 6 slices, 5 animals (CTRL); 5 slices, 5 animals (LTP). **B.** Puromycin labeling was sensitive to inhibitors of protein synthesis, anisomycin and cycloheximide. CTRL: 1.0 ± 0.03 v. ANISO: 0.45 ± 0.10 v. CHX: 1.32 ± 0.05, One Way ANOVA, F[2,11]= 41.18, p < 0.0001, n = 4 slices, 4 animals. **C.** Slices without secondary antibody or lacking puromycin displayed similarly low background levels indicating specificity of puromycin primary antibody. CTRL(+ puromycin): 1054 ± 58 v. -puromycin: 501 ± 0.54 v. – secondary: 512 ± 5.2. One-Way ANOVA, F[2,12] = 89.39, p < 0.0001, n = 5 slices per condition. Points represent individual slices and are normalized to mean of CTRL. **D.** Fmr1 cKO did not increase in PMY labeling in stratum radiatum. WT: 1.0 ± 0.03 v. WT + LTP: 1.17 ± 0.08 v Fmr1 cKO: 1.13 ± 0.07 v. Fmr1 cKO+ LTP: 1.01 ± 0.06 (Mean ± S.E.M.); Two-Way ANOVA with Tukey's test for Multiple Comparisons, Interaction: F[1,58] = 3.72, p = 0.06. n = 18,14, 15, 16 slices respectively. Points represent individual slices and are normalized to mean of WT.

Supp. Figure 4

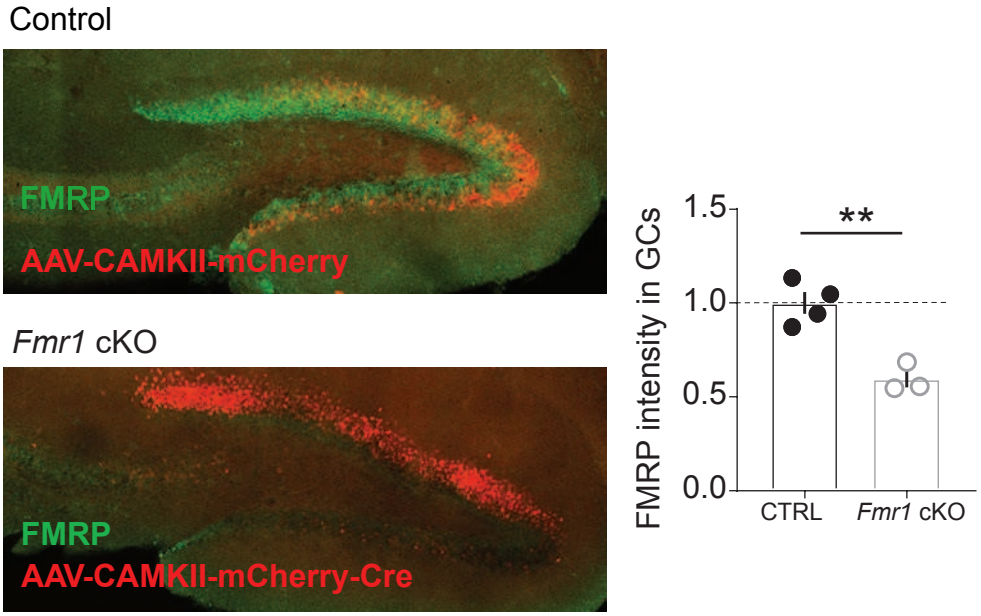

Supp. Figure 4 (related to Figure 6) FMRP was effectively reduced using viral injection of AAV-Cre *Fmr1*$^{fl/fl}$ injected with AAV5-CAMKII-mCherry +/- Cre. FMRP intensity measured by antibody labeling in mCherry-positive GCs was reduced by Cre expression. CTRL: 4 Fmr1 cKO: 3 mice; Two-sample t-test, p = 0.0035

Supp. Figure 5

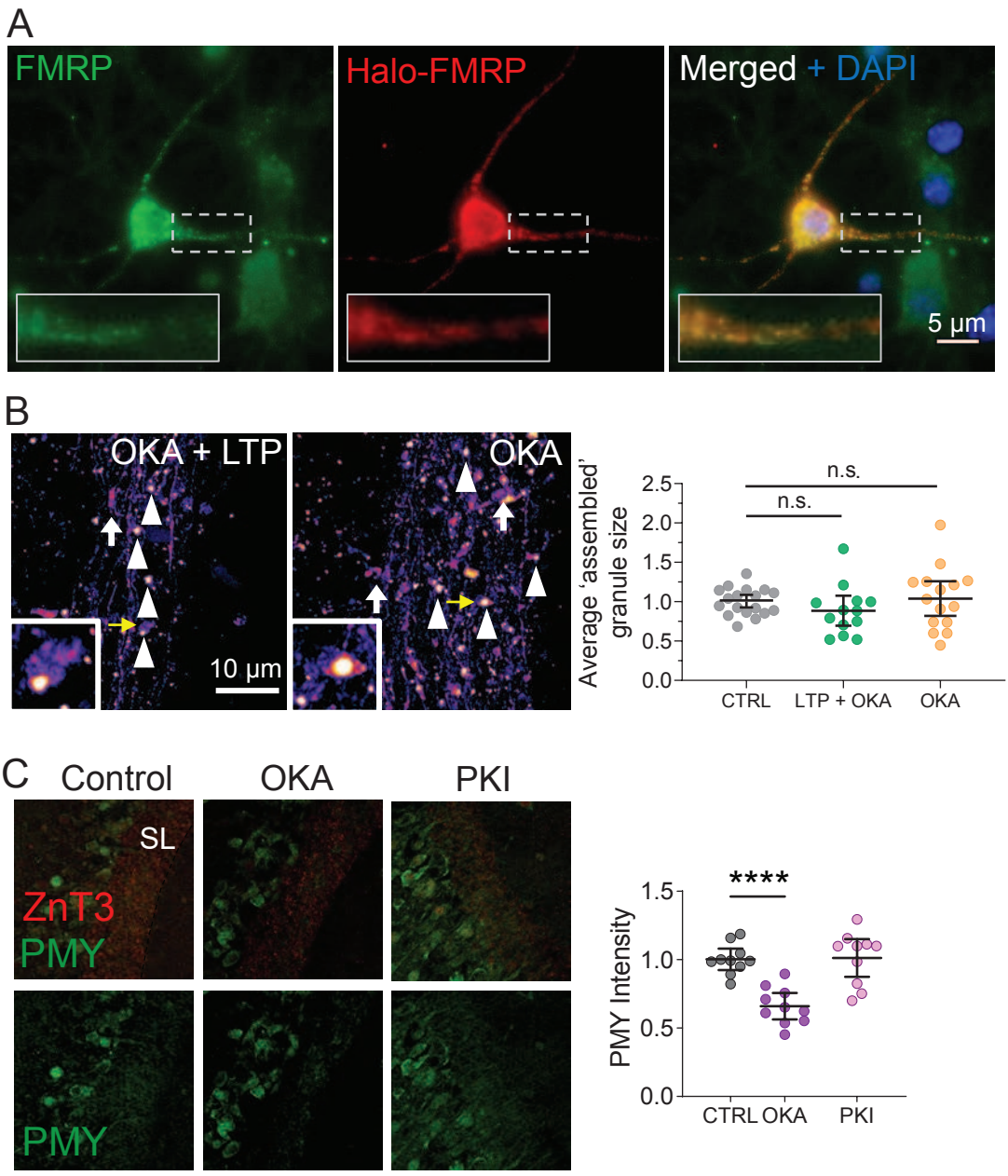

Supp. Figure 5. (related to Figure 7) Characterization of Halo-FMRP construct and mechanism of FMRP granule regulation by MF-LTP A. Endogenous FMRP (left) and FMRP-Halotag (right) colocalized in dendrites of cultured hippocampal neurons. Scale bar denotes 5 µm. **B.** Activity-dependent FMRP Halotag granule dissembly was regulated by PP2A. Application of okadaic acid (OKA, 25 nM, 30 min) blocked LTP induced decrease in granule size and had no effect on basal granule size. CTRL: 1.00 ± 0.04 v. LTP + OKA: 0.89 ± 0.09 v. OKA: 1.04 ± 0.10 (Mean ± S.E.M. normalized to control); One-Way ANOVA with Tukey's test for Multiple Comparisons, $F[2,43] = 0.98$, $p = 0.38$; n = 18, 13, 15 slices respectively. Points represent individual slices and are normalized to mean of WT. **C.** PP2A inhibition with OKA, but not PKA inhibition with PKI, significantly reduced baseline protein synthesis. CTRL: 1.00 ± 0.03 v. OKA: 0.66 ± 0.04 v. PKI: 1.01 ± 0.06 (Mean ± S.E.M. normalized to control); One-Way ANOVA with Tukey's test for Multiple Comparisons, $F[2,27] = 17.94$, $p < 0.0001$; n = 10 slices per condition. Points represent individual slices and are normalized to mean of WT.

Supp. Figure 6

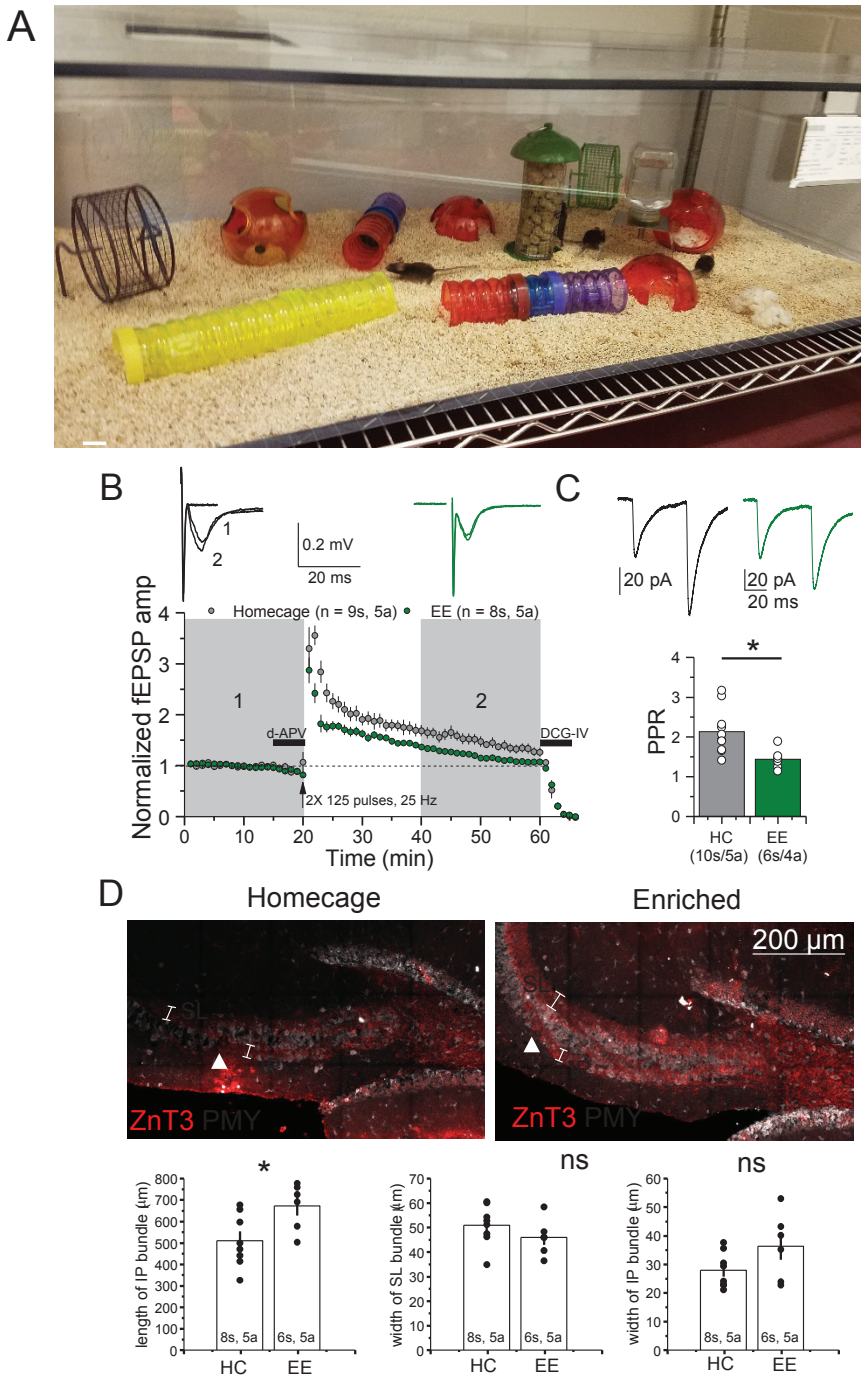

Supp. Figure 6. (related to Figure 8) EE alters the mossy fiber bundle A. Enriched environment (EE) setup. Mice were housed in a large plexiglass enclosure in groups of 5 or more and have access to running wheels, tubes, toys and ample nesting supplies. Objects are rearranged every other day. **B.** Extracellular field recordings demonstrate EE occluded MF-LTP. HC: 1.44 ± 0.09 v. EE: 1.18 ± 0.04; Two sample t-test, p = 0.023 **C.** Whole cell recording showed PPR was reduced at baseline in EE mice. HC: 2.14 ± 0.18 v. EE: 1.44 ± 0.11; Two sample t-test, p = 0.01 **D.** Histology of mossy fiber tract revealed expansion of the infrapyramidal bundle in EE, while other measures of gross anatomy of MF tract were unaffected. Arrowheads indicate approximate end of IP, brackets show the width of SL and IP. IP Length of IP: HC: 510.2 ± 43.6 v. EE: 672.70 ± 44.5, Two-sample t-test, p = 0.0251. Width of SL: HC: 50.97 ± 2.94 v. EE: 46.02 ± 3.06, Two-sample t-test, p = 0.27. Width of IP: HC: 28.02 ± 2.21 v. EE: 36.37 ± 4.76, Two-sample t-test, p = 0.11.